EVALUATION OF HEAT TRANSFER COEFFICIENTS FOR AN IMPINGEMENT COOLING CASCADE: EXPERIMENTAL CHALLENGES AND PRELIMINARY RESULTS

Michele Gaffuri, Alexandros Terzis, Peter Ott
EPFL - Swiss Federal Institute of Technology
Group of Thermal Turbomachinery (GTT)
1015 Lausanne, Switzerland
michele.gaffuri@epfl.ch

Stefan Retzko, Marc Henze
ANSALDO Energia Switzerland
Römerstrasse 36
5401 Baden, Switzerland

ABSTRACT

In this paper, a modification of the widely used transient liquid crystal heat transfer measurement technique for impingement cooling is presented, in which a constant heat flux at the surface is used to drive the experiment, instead of a step change in the flow temperature. This method, already employed for film cooling, is used for the first time in a narrow impingement channel of an impingement cooling cascade which is characterized by complex and three dimensional vortical structures. The results are compared to the traditional heater mesh method (i.e. a temperature step in the flow drives the experiment). With both methods similar results are obtained, with the associated differences that can be attributed to entrainment effects or different surface roughness. An uncertainty analysis shows also that a transient experiment with constant surface heat flux improves the accuracy in the high heat transfer regions, e.g. stagnation points, which are the most uncertain regions in the heater mesh method.

NOMENCLATURE

DC   direct current
Nu   Nusselt number [-]
PMMA   Poly(methyl methacrylate)
Pr   Prandtl number [-]
Re   Reynolds number [-]

A target plate surface area [m^2]
D jet diameter [m]
h heat transfer coefficient [$W/(m^2K)$]
q heat flux [W/m^2]
Q power [W]
T temperature [K]
T_0 initial/ambient temperature [K]
T_g hot gas temperature [K]
T_{LC} liquid crystal event temperature [K]
X jet spacing [m]
Y channel width [m]
z depth coordinate [m]
Z channel height [m]
α thermal diffusivity [m^2/s]

INTRODUCTION

Impingement channels are widely used for the cooling of gas turbine vanes and blades, due to the very high local heat transfer coefficients that can be achieved in the stagnation zones. In modern integrally cast turbine airfoils, narrow impingement cooling channels [1] can be created where the coolant is injected within the wall rather than the hollow of the airfoil. This generates a double-wall cooling arrangement [2], as shown in the left part of Figure 1. In-wall cooling technologies, which may also include small pre-film impingement chambers [3], are able to reduce metal temperatures by as much as 100K.

Narrow impingement cooling channels consist of single or double rows of several cooling jets (see right part of Figure 1), while the small wall thickness of a typical airfoil ($\sim2mm$) dictates significant heat transfer for all the internal surfaces of the cavity. These integrally cast impingement channels are radially oriented in the turbine airfoil which can include a plurality of similar cavities ensuring a homogeneous distribution of the material temperature. Due to the small passage areas, crossflow effects are of great importance for the optimization of narrow impingement schemes because the spent air of the jets interferes with the other walls of the channel providing complex flow structures and a degradation of the heat transfer performance for the downstream jets. Attempts to regulate the generated crossflow in narrow impingement channels include jet hole staggering positions [4], varying jet diameters in the streamwise direction [5] as well as divergent channel geometries [6].

In order to gain additional efficiency, the narrow channels can be used in a cascade impingement scheme where the air from one cavity could be used for impingement in the following channel through an intermediate plenum chamber, as shown in Figure 3.

Experimental tests on impingement channels are generally carried out using the transient liquid
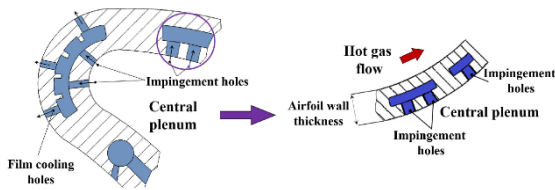
Figure 1: Narrow impingement channels in a double wall-cooling configuration.

crystal technique [7]: starting at ambient temperature, the flow is suddenly heated to a higher temperature, and the temperature evolution of the surface is determined by watching the color change of a thermochromic liquid crystal coating. The convective heat transfer coefficient is then derived by using the one-dimensional heat conduction equation with a semi-infinite wall assumption.

In a cascade impingement scheme, however, the determination of the gas temperature, needed for the derivation of the heat transfer coefficient, is problematic: on one hand, the flow temperature can be non-uniform between the various jets of the downstream array; on the other hand complex schemes can include bypasses from one chamber to the other, so that the actual local hot gas temperature depends on the mixing of 2 or more flows, which can be at different temperatures. Additionally, whereas the temperature increase can be considered an ideal step in the first channel, it is slower for the jets of the second impingement: the post-processing of the results would be more complex and involves either using Duhamel's principle or relying on analytical solutions for different gas temperature evolutions.

To overcome these issues, the experimental technique has been modified by including a surface heat flux generated by a heater foil attached on the target plate; the flow is kept at ambient temperature and the heat equation modified by adding a source term in the boundary condition. This method has already been successfully applied for the evaluation of film cooling ([8]-[9]).

In the present work, the modified technique is validated in the first impingement channel, where it can reliably be compared to the standard measurement technique. In the future, the technique will be used to assess the thermal performances of the complete cascading impingement channel.

TOOLS AND METHODS
Test facility

EPFL's heat transfer test facility (see [7]) has been adapted in order to evaluate the heat transfer performances of an impingement cascade system. It consists of a bell mouth inlet which leads air into a plenum, on top of which is located the cascading impingement test geometry. The outlet of the test geometry is connected to the driving vacuum pump via a plastic, vacuum resistant tubing.

Upstream of the plenum, a stainless steel mesh is used to heat the passing air via Joule heating; electrical power is provided by two DC power supplies which can achieve 30 kW (60V, 500 A).

For the new technique with a surface energy source, an aluminum tape is attached to the target surface, and is clamped on both ends using copper bars to connect the electrical power, which is provided by a 50V, 128A DC power supply. Being a good electricity conductor, aluminum is not a priori the best candidate for a heater foil, because it requires high current to deliver the required power. However, it comes in tape form and is thus much easier to install than e.g. a stainless steel foil. Indeed, a non-perfect attachment of the foil on the target surface will result in a noticeable error in the evaluation of the heat transfer coefficient h.

The mass flow is measured via a laminar flow element located upstream of the pump. Type K thermocouples are mounted in the plenum, upstream of each jet, to evaluate the jet temperature. Pressure taps in the plenum and at the channel outlet allow for the evaluation of the channel's discharge factor.

The target surfaces are made of PMMA and painted with thermochromic liquid crystals (Hallcrest SPN100/R35C1W) and black paint. Where applicable, the aluminum foil is glued to the plate after the two layers of paint.

The power generated by the foil is computed by the relation $Q=RI^2$. The current I is read directly on the power supply and is constant, while the resistance of the foil is measured prior to the tests at ambient temperature and at the liquid crystals event temperature; the average of this 2 measurements is used for the power computation.
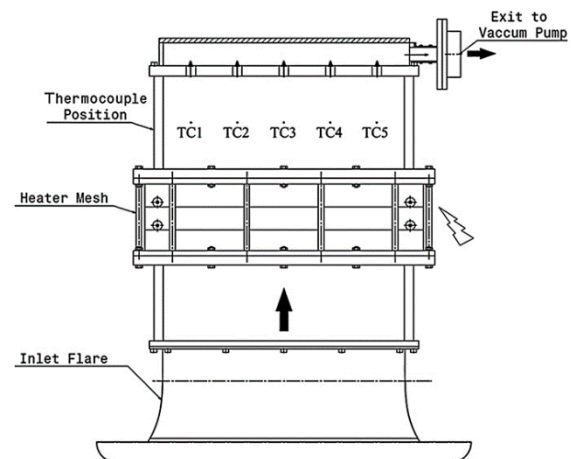

Figure 2: Schematics of the test rig, with a single narrow impingement channel installed on top.

Transient measurement technique – heater mesh

The transient liquid crystal technique employed here is described in detail in [7]. Essentially, the flow

and the test geometry are initially at temperature T_0. At the time t=0, the air is suddenly brought to a higher temperature T_g by circulating electrical current in the heater mesh, and the temperature evolution of the target plate can be tracked by monitoring the color change of the liquid crystal paint, whose color-temperature relationship has been previously determined by calibration. In order to derive the heat transfer coefficient, one has to solve the one-dimensional heat conduction equation with a semi-infinite wall assumption:

$$\frac{\partial^2 T(z,t)}{\partial z^2} = \frac{1}{\alpha} \frac{\partial T(z,t)}{\partial t}$$

with the initial condition:

$$T(z,0) = T_{amb}$$

and the boundary conditions:

$$-k\frac{\partial T(0,t)}{\partial z} = h[T_g - T(0,t)]$$
$$T(\infty,t) = T_{amb}$$

In the above α and k are the thermal diffusivity and thermal conductivity of the plate, respectively. It can be shown **[11]** that the general solution of this problem is:

$$\frac{T(z,t) - T_0}{T_g - T_0} = \text{erfc}\left(\frac{z}{2\sqrt{\alpha t}}\right) - e^{\left(\frac{hz}{k} + \frac{h^2\alpha t}{k^2}\right)}\text{erfc}\left(\frac{z}{2\sqrt{\alpha t}} + \frac{h\sqrt{\alpha t}}{k}\right)$$

If the time t_{LC} required to reach a certain temperature T_{LC} at the surface (z = 0) is known, the solution becomes

$$\frac{T_{LC} - T_0}{T_g - T_0} = 1 - e^{\left(\frac{h^2\alpha t_{LC}}{k^2}\right)}\text{erfc}\left(\frac{h\sqrt{\alpha t_{LC}}}{k}\right)$$

This equation can be solved numerically to find h for each pixel of the image. It has to be noted that the equation can similarly be solved for $z \neq 0$ if the thickness of the black paint has to be considered and its thermal properties are similar to those of the plate.

Transient measurement technique – heater foil

The heater foil technique applied here is similar to the one described in **[10]**. Instead of performing a step change in the fluid temperature, at time t=0, as in the previous method, an electrical current is passed through the heater foil, generating a power Q, which provides a constant local surface heat flux q=Q/A, where A is the foil area.

The same one-dimensional semi-infinite heat equation is considered, but now the boundary condition is modified to include the heat flux q:

$$-k\frac{\partial T(0,t)}{\partial z} = q - h[T(0,t) - T_g]$$

Considering a constant gas temperature, T_g=T_0, the differential equation can be solved **[11]** as follows:

$$h\frac{T(z,t) - T_0}{q} = \text{erfc}\left(\frac{z}{2\sqrt{\alpha t}}\right) - e^{\left(\frac{hz}{k} + \frac{h^2\alpha t}{k^2}\right)}\text{erfc}\left(\frac{z}{2\sqrt{\alpha t}} + \frac{h\sqrt{\alpha t}}{k}\right)$$

Again, after the determination of the time t_{LC} required to reach the temperature T_{LC}, the equation can be solved numerically for h at the required depth z, consisting of the thickness of the black paint plus the thickness of the glue used to attach the foil to the surface.

Test geometry

The geometry under consideration is a cascading impingement geometry with 2 identical channels with rectangular section Y/D=5 and Z/D=3. Each channel contains five circular impingement holes with uniform spacing X/D=5.

After the first impingement, the air discharges through an obround hole in a second plenum where it can be used in the second impingement channel. All surfaces are made of PMMA to allow for optical access and to satisfy the one-dimensional approach. The plates have a thickness of 20 *mm* in order to comply with the semi-infinite hypothesis in the resolution of the heat equation for all typical measurement durations.

The target plates have slots to insert copper bars, which are used to clamp the heater foils and connect them to the power supply.
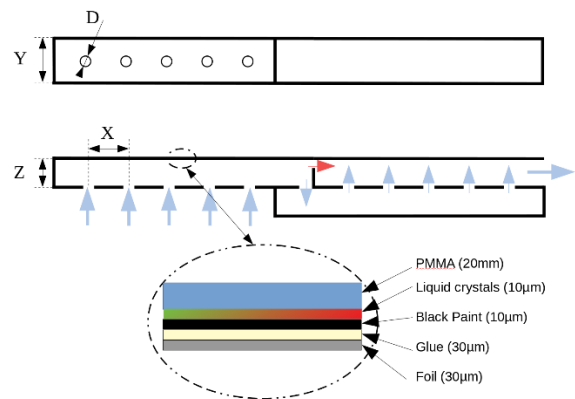

Figure 3: Bottom view and side view of the impingement cooling cascade tested. Blue arrows show the main coolant flow, while the red arrow shows the bypass flow. Below a sketch (not to scale) of the target surface coatings with their respective thicknesses.

Calibration

All the thermocouples used are calibrated together in a thermostatic liquid bath (Lauda E4S) with the temperature determined using a precision thermometer (Omega DP 251). The liquid crystal indication temperature T_{LC} is determined by recirculating constant temperature water from the liquid bath in an insulated box with a PMMA top. Inside the box, a copper block is instrumented with calibrated thermocouples and painted on its top surface with a layer of liquid crystals above a layer of black paint. A snapshot of the top surface is taken when the temperature given by the thermocouples is stable, after which the temperature of the recirculating liquid bath is increased and the process repeated.

After analyzing the images, the temperature associated with the maximum green intensity can be determined, see Figure 4.
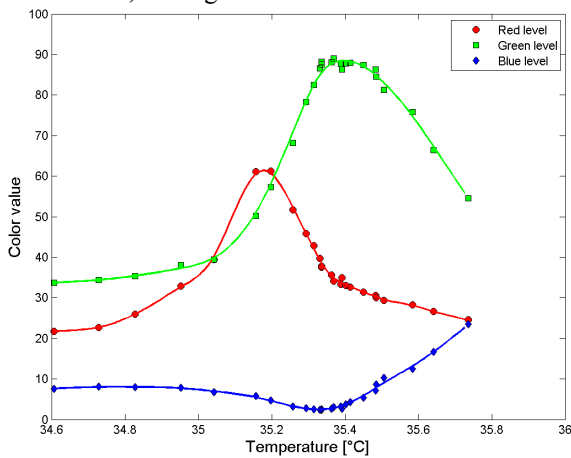

Figure 4: RGB values of the liquid crystals as a function of the temperature. Solid lines are spline fittings of the data.

RESULTS

An illustrative result of the heater foil method is presented in Figure 5, where the heat transfer coefficient is visualized with a color scale. The heat transfer spatial evolution is quite smooth, and this is only possible with a perfect attachment of the foil on the surface; even small glitches in the foil attachment (waviness, air bubbles) are noticeable in the heat transfer distribution. At the downstream wall the threaded holes used to fix the copper bars to the target plate are clearly noticeable. It is unclear what causes the high heat transfer region in the right end side. It could be due to the fact that some heat generated on the foil is conducted to the copper bars clamping the foil.
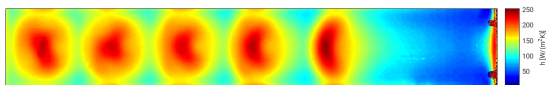

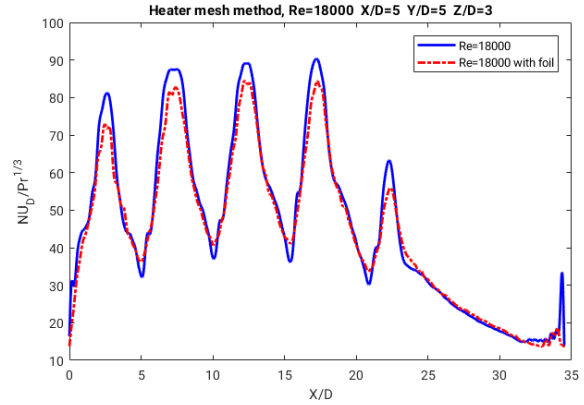*Figure 5: Heat transfer coefficient obtained after pros-processing the heater foil test data (Re=32000).*

Figure 6: Influence of the presence of the foil on the heat transfer. Heater mesh method at Re=18000 with and without foil attached; crossflow from left to right.
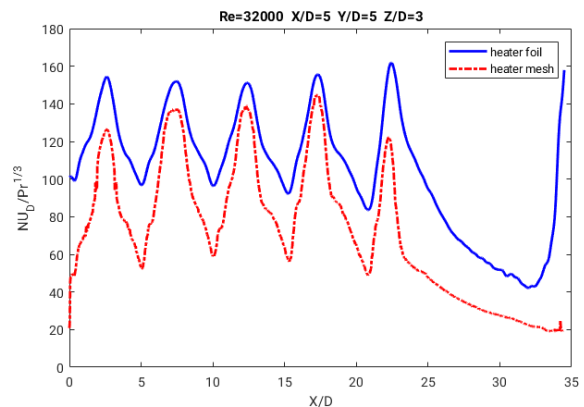

Figure 7: Comparison of the heat transfer predicted using the heater foil and the heater mesh method. Crossflow from left to right.

To evaluate the suitability of the heater foil method, in a first step the influence of the foil on the flow and heat transfer is evaluated by performing tests using the heater mesh method with and without the foil attached; in the latter case, the resolution of the heat equation is solved for z=40μm, to take into account the thickness of the glue used to attach the foil.

A comparison of the Nusselt number at the center line of the first target plate is shown in Figure 6. It can be noted that with the foil, the heat transfer in the stagnation region is lower than without the foil, while it is slightly higher for the low heat transfer regions in between the jets (local minima). This could be an indication of lateral conduction within the aluminum foil, which has high thermal conductivity. A discrepancy in the stagnation region could also be caused by a different surface texture between the black paint layer and the aluminum foil.

Figure 7 shows the Nusselt number over the Prandtl number to the power of 1/3, evaluated with both experimental methods. The heater foil method tends to overestimate the heat transfer levels compared to the heater mesh method. This is expected due to the entrainment effect (**[12-13]**)

present in the heater mesh method: in this case, the jet is at a higher temperature than the fluid initially present inside the channel, which is at ambient temperature. The entrainment of ambient air reduces the heat transfer. Since the heat transfer coefficient is defined using the jet temperature as the reference hot temperature, the results are lower than for the heater foil case, where the entrained air is at the same temperature as the jet air.

The stagnation point Nusselt number evolution is different in the two methods. In particular, the heater mesh method shows noticeably lower heat transfer for the last jet. This could be due to the fact that the last impingement hole is very close to the border of the plenum, and possibly at the edge of the thermal boundary layer of the plenum flow.

Uncertainty analysis

The overall uncertainty of the experiments can be estimated using the root sum square (RSS) method [15]. The 95% confidence interval of the measured parameters, supposed to be statistically independent and normally distributed, can be combined to estimate the uncertainty on the heat transfer coefficient (Δh) as follows:

$$\Delta h^2 = \sum_i \left(\frac{\partial h}{\partial x_i}\right)^2 \Delta x_i^2$$

Where x_i are the uncertain parameters needed for the computation of h.

A detailed uncertainty analysis for the transient heater mesh technique using this setup is available in [14].

Figure 8 shows the relative uncertainty along the channel center line. For the heater mesh technique the relative error is approximately 14% at the stagnation point and drops to 8% in the low heat transfer regions, while the heater foil method minimizes the error at the stagnation point (around 5%) and increases in the low heat transfer regions up to 15%.
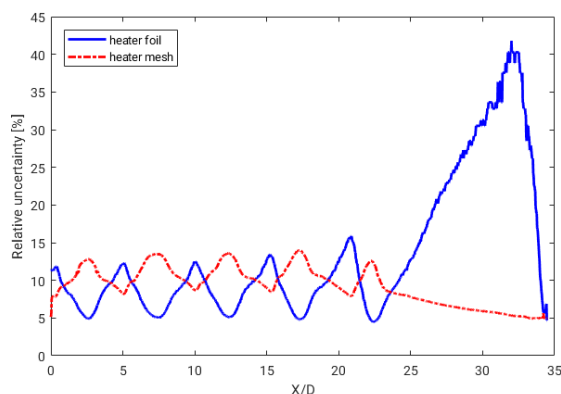

Figure 8: 95% confidence interval for the heat transfer coefficient in the center line of the channel at Re=32000, expressed as a percentage of the local heat transfer coefficient.

An increased accuracy in the stagnation region has thus to be traded off by having higher uncertainty in the low heat transfer regions. In the transition zone, characterized by very low heat transfer, the relative uncertainty of the heater foil method increases noticeably, due to the fact that the liquid crystal event temperature is reached very fast, and thus the relative uncertainty on the time is high.

In Figure 9 the contribution, for the heater foil method, of each individual term to the overall uncertainty is shown for two different locations: the stagnation region and the wall jet region, in-between two stagnation points. By far, the biggest contributors to the overall uncertainty are the heat flux and the material properties (thermal conductivity, thermal diffusivity). Indeed, the results are very sensitive to the heat flux variation, and an accurate measurement of the applied power is difficult for two reasons:

1. Due to the low resistivity of the foil material, the resistance cannot be measured at the power supply, because the resistance of the cables is of the same order of magnitude as the resistance of the foil.
2. The experiment is performed at constant current. The resistance of the foil increases with the foil temperature, causing the heat flux to (slightly) vary over time.
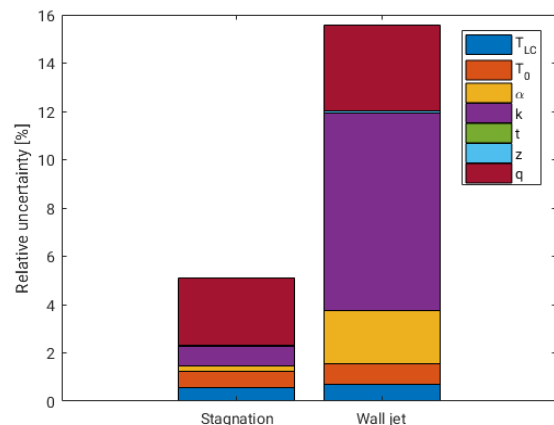

Figure 9: Relative contribution of each parameter to the overall uncertainty of the heat transfer coefficient for 2 locations on the center line of the channel.

It has to be noted that the dependence on the heat flux value can be avoided if one also considers the cooling part of the experiment, i.e. when the heat flux is suddenly turned off (or reduced). A priori, this has the potential to increase the accuracy of the experiments.

CONCLUSIONS AND OUTLOOK

A modification of the transient liquid crystal thermography experiment by using heater foils on the target surface has been presented. It allows for an increased accuracy in the stagnation regions of narrow impinging jet channels. The method has the

advantage of being applicable in cases where a sharp temperature step in the flow cannot be achieved.

In the future, the accuracy of the method in low heat transfer regions has to be increased. Better control of the heat flux level (better instrumentation, a higher resistivity material for the foil), or taking into account the cooling phase of the experiment could reduce the uncertainty related to the heat flux determination.

ACKNOWLEDGMENTS

REFERENCES

[1] Terzis, A., Ott, P., von Wolfersdorf, J., Weigand, B., and Cochet, M., 2014, "Detailed Heat Transfer Distributions of Narrow Impingement Channels for Cast-In Turbine Airfoils," **ASME J. Turbomach.**, 136(9), p. 091011.

[2] Lutum, E., Semmler, K., and von Wolfersdorf, J., 2002, "Cooled Blade for a Gas Turbine," **U.S. Patent**, No. 6,379,118 B2

[3] Gillespie, D. R. H., Wang, Z., Ireland, P. T., and Kohler, S. T., 1998, "Full Surface Local Heat Transfer Coefficient Measurements in a Model of an Integrally Cast Impingement Cooling Geometry," **ASME J. Turbomach.**, 120(1), pp. 92–99.

[4] Terzis, A., Wagner, G., von Wolfersdorf, J., Ott, P., and Weigand, B., 2014, "Effect of Hole Staggering on the Cooling Performance of Narrow Impingement Channels Using the Transient Liquid Crystal Technique," **ASME J. Heat Transfer**, 136(7), p. 071701.

[5] Terzis, A., Ott, P., Cochet, M., von Wolfersdorf, J., and Weigand, B., 2015, "Effect of Varying Jet Diameter on the Heat Transfer Distributions of Narrow Impingement Channels," **ASME J. Turbomach.**, 137(2), p. 021004.

[6] Terzis, A., Skourides, C., Ott, P., von Wolfersdorf, J., and Weigand, B., 2016, "Aerothermal investigation of a single row divergent narrow impingement channel by particle image velocimetry and liquid crystal thermography," **ASME J. Turbomach.** 138(5), p. 051003

[7] Terzis, A., Bontitsopoulos, S., Ott, P., von Wolfersdorf, J., & Kalfas, A. I., 2016, "Improved accuracy in jet impingement heat transfer experiments considering the layer thicknesses of a triple thermochromic liquid crystal coating", **ASME J. Turbomach.** 138(2), 021003.

[8] Vogel, G., Graf, A. B. A., Von Wolfersdorf, J., and Weigand, B., "A novel transient heater-foil technique for liquid crystal experiments on film-cooled surfaces" **ASME J. Turbomach.**, 125(3), 529-537.

[9] Jonsson, M., Charbonnier, D., Ott, P., and von Wolfersdorf, J., "Application of the transient heater foil technique for heat transfer and film cooling effectiveness measurements on a turbine vane endwall", Proccedings of the **ASME Turbo Expo 2008** (pp. 443-453).

[10] Von Wolfersdorf, J., Hoecker, R., & Sattelmayer, T., 1993, "A hybrid transient step-heating heat transfer measurement technique using heater foils and liquid-crystal thermography", **ASME J. Heat Transfer**, 115(2), 319-324.

[11] Carslaw, H. S., & Jaeger, J. C., 1959, "Conduction of heat in solids", Oxford Science Publications, Oxford, England.

[12] Goldstein, R. J., Sobolik, K. A., & Seol, W. S., 1990, "Effect of entrainment on the heat transfer to a heated circular air jet impinging on a flat surface." **ASME J. Heat Transfer**, 112(3), pp. 608-611.

[13] Hollworth, B. R., & Gero, L. R., 1985, Entrainment effects on impingement heat transfer: part II—local heat transfer measurements. **ASME J. Heat Transfer**, 107(4), pp. 910-915.

[14] Terzis A., Detailed heat transfer distributions of narrow impingement channels for integrally cast turbine airfoils," Ph.D Thesis N° 6277, EPFL, Switzerland, 2014.

[15] Kline, S. J. & McClintock, F. A., Describing Uncertainties in Single-Sample Experiments, **Mechanical Engineering**, Vol. 75, No. 1, 1953, pp. 3-8.